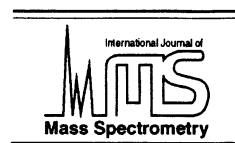




ELSEVIER

International Journal of Mass Spectrometry 201 (2000) 215–231



Cu^+ reactivity trends in sp , sp^2 , and sp^3 nitrogen, phosphorus, and arsenic containing bases

Alberto Luna,^a Manuel Alcamí,^a Otilia Mó,^a Manuel Mánuez^a

Departamento de Química, C-9, Universidad Autónoma de Madrid, Cantoblanco, 28049, Madrid, Spain

Received 29 September 1999; accepted 20 December 1999

Abstract

Density functional theory (DFT) has been used to analyze the reactivity trends of sp , sp^2 , and sp^3 nitrogen bases with respect to their phosphorus and arsenic analogues, both when the reference acid is H^+ or Cu^+ . Geometries were fully optimized at the B3LYP/6-311G(*d*, *p*) level and the final energies were obtained in B3LYP/6-311 + G(2*df*, 2*p*) single point calculations. For some model systems the G2 molecular orbital theory was used to assess the reliability of the DFT approach used. Significant differences in the reactivity trends of the nitrogen bases with respect to their phosphorus and arsenic analogues have been found. While for $\text{H}_2\text{C}=\text{NH}$ only the nitrogen attached species is stable, for $\text{H}_2\text{C}=\text{PH}$ and $\text{H}_2\text{C}=\text{AsH}$ both, the species in which the cation is bonded to the heteroatom and the carbon attached structures are local minima of the potential energy surface. Furthermore, for the arsenic derivative the latter is the most stable form. Similarly, while for HCN only the nitrogen attached species is stable for HCP and HCAs only the carbon attached structures are found. The basicities of XH_3 and CH_3XH_2 were also studied for comparison. Methyl substituent effects for phosphorus and arsenic compounds are larger than for the corresponding nitrogen derivative. Proton affinities and Cu^+ binding energies are linearly correlated, although the slope of the correlation for phosphorus and arsenic derivatives is significantly different from that of nitrogen bases. The unsaturated systems are systematically less basic than the corresponding saturated counterparts. The observed differences in the reactivity trends reflect significant dissimilarities in the charge redistribution undergone by the neutral when it interacts with the attaching ion, which are also mirrored in the optimized geometries and in the shiftings of the harmonic stretching frequencies. (Int J Mass Spectrom 201 (2000) 215–231) © 2000 Elsevier Science B.V.

Keywords: Cu^+ reactivity trends; Nitrogen; Phosphorus and arsenic bases; DFT calculations

1. Introduction

The gas-phase ion chemistry is an area which has witnessed an impressive development in the last decades [1]. Of particular increasing interest have been the reactions of gas-phase ions with neutral molecules, due, in part, to a growing awareness of the

importance of these ion-molecule interactions. A great deal of attention was initially devoted, for obvious reasons, to protonation processes in the gas-phase and nowadays the scale of proton affinities includes hundreds of compounds [2]. More recently, these studies were extended to other gas-phase cations, in particular to metal monocations [3], so that in many cases it was possible to establish a relationship between gas-phase metal cation binding energies and proton affinities [4]. In this scenario the role played by

* Corresponding author. E-mail: manuel.yanez@uam.es

the theoretical methods was crucial for several reasons: on the one hand, the use of *ab initio* molecular orbital techniques was, and still is in many instances, the only reliable tool to obtain information on the structure of the molecular ions formed in the aforementioned ion–molecule reactions. Hence, very often, our knowledge on the active sites of different neutral compounds is based on the agreement between the theoretically estimated values for the ion–molecule binding energies and the experimental ones obtained using different experimental techniques. On the other hand, a rationalization of the unimolecular decomposition of the molecular ions formed in ion–molecule reactions requires a good and detailed knowledge of the potential energy surface, which can be only attained on theoretical grounds. This was the origin of a fruitful interplay between theory and experiment which resulted in a deeper understanding of the mechanisms associated with bond activation and catalytic processes [5]. One driving force behind the application of *ab initio* calculations in this field has been the ability to obtain reliable thermochemical quantities, such as enthalpies of formation, ionization potentials, proton and electron affinities, etc. Actually, the so called high-level *ab initio* techniques are the only alternative to estimate the heats of formation of many species that, in spite of its very low stability [6], can be important to understand the chemistry in extreme conditions environments, as the interstellar space.

In the course of the last decade there has been a substantial progress in the refinement of density functionals. As a consequence, these methods are nowadays currently used as an alternative to *ab initio* calculations. The fact that density functional theory (DFT) calculations are less computationally demanding than the standard *ab initio* procedures has permitted to extend the exploration of the potential energy surfaces to larger and larger systems.

In this context, we have devoted some efforts to the study of the gas-phase reactions of organic compounds with different metal monocations [7] and in the last years particular attention has been focused [8] on reactions involving Cu^+ with nitrogen and oxygen bases. The aim of this article is to study the intrinsic reactivity of *sp*, *sp*², and *sp*³ phosphorus and arsenic

containing bases with respect to Cu^+ and to compare it with the reactivity exhibited by the nitrogen containing analogs, which was previously studied [9], in an effort to establish the reactivity trends down the group. Since there is an almost complete lack of data regarding the intrinsic reactivity of phosphorus and arsenic bases, we have also considered it of interest to compare their Cu^+ binding energies with the corresponding proton affinities.

2. Computational details

The theoretical treatment of the different systems included in this work was performed by using the B3LYP density functional approach as implemented in the GAUSSIAN-94 series of programs [10]. This method has been found to be quite reliable as far as the description of metal cation–neutral complexes is concerned [11], in particular when Cu^+ ions are involved [8,9,12]. The B3LYP approach is a hybrid method which includes the Becke's three parameter nonlocal exchange potential [13] with the nonlocal correlation functional of Lee et al. [14]. The geometries of the different species under consideration were optimized using the all electron basis of Wachters-Hay [15] for Cu and the 6-311G(*d*, *p*) basis set for the remaining atoms of the system. The harmonic vibrational frequencies of the different structures investigated have been calculated at the same level of theory used for their geometry optimization in order to identify the local minima and the transition states (TS), as well as to estimate the corresponding zero point energy (ZPE) corrections. The final energies of the different species under study were obtained in B3LYP/6-311 + G(2*df*, 2*p*) single point calculations at the aforementioned B3LYP/6-311G(*d*, *p*) optimized geometries. This level of theory has been shown [9] to provide Cu^+ binding energies for nitrogen bases which are in reasonably good agreement with those estimated in the framework of the G2 theory [16] and with recent experimental values [17]. It is worth noting that in these DFT calculations the largest basis set expansion used includes only two sets of *d* polarization functions rather than three as in the

G2 formalism [16], because, as shown in [9], the reduction in the number of the d polarization functions has a negligible effect on the calculated binding energies but implies a significant saving in the computation time. It must be also mentioned that, although for the sake of simplicity we maintain the nomenclature “6-311 + G(2df, 2p)” for all the atoms, for Cu this basis set corresponds to the (14s9p5d/9s5p3d) basis of Wachters-Hay supplemented with a set of (1s2p1d) diffuse functions and with two sets of f functions (rather than d functions) and one set of g functions (rather than f functions).

Since to the best of our knowledge, no experimental values on the Cu^+ binding energies have been reported for the P and As containing compounds included in our study, and in order to assess the reliability of our DFT estimates when dealing with second- and third-row bases we shall also use the G2 theory [16] which, as mentioned in the introduction, has been extremely successful at predicting many thermochemical magnitudes with an accuracy which is often better than 2 kcal/mol, and which has been recently extended [18] to the treatment of molecules containing third-row atoms. For this purpose we have chosen PH_3 and AsH_3 as suitable model systems. For the sake of consistency with our DFT calculations, the geometries were optimized using a 6-311G(d , p) basis set, rather than the 6-31G(d) normally used in the standard G2 procedure. The harmonic vibrational frequencies were also obtained at the MP2(full)/6-311G(d , p) level of theory and the corresponding ZPE corrections were scaled by the empirical factor 0.93 [19].

The bonding characteristics of the different species have been investigated by using the atoms in molecules (AIM) theory of Bader [20]. For this purpose, we have located the bond critical points, i.e. points where the electron density function, $\rho(\mathbf{r})$, is minimum along the bond path and maximum in the other two directions. We have also calculated the energy density, $H(\mathbf{r})$, at each bond critical point. In general, negative values of $H(\mathbf{r})$ denote the existence of stabilizing charge concentrations within the bonding region, which are associated with covalent interactions. The AIM analysis was performed using the AIMPAC series of programs [21].

3. Results and discussion

3.1. Structures and charge distributions

The optimized geometries of the different phosphorus and arsenic containing bases and their Cu^+ complexes have been schematized in Fig. 1. It is worth mentioning that the calculated geometries are in excellent agreement with experiment, whenever this information is available. For the sake of comparison Fig. 1 includes also the optimized geometries of the nitrogen containing analogs taken from [9].

As expected in all $\text{XH}_3\text{--Cu}^+$ ($X = \text{N}, \text{P}, \text{As}$) complexes the C_{3v} symmetry of the neutral is preserved. However, the geometrical changes induced in ammonia by the attachment of the metal cation are opposite to those observed in phosphine or arsine. While in ammonia a slight decrease of the HNH bond angles takes place, in PH_3 and AsH_3 the corresponding bond angles significantly increase. Similarly, while the N–H bond lengths of ammonia increase upon complexation with Cu^+ , the P–H and the As–H bonds shorten. Similar effects can be observed in methylamine, methylphosphine, and methylarsine.

Significant dissimilarities are also observed between sp^2 nitrogen bases and their phosphorus and arsenic analogs. Actually, it can be seen, for example, that while for imine, $\text{H}_2\text{C=NH}$, only the nitrogen attached Cu^+ complex is stable, for $\text{H}_2\text{C=PH}$ and $\text{H}_2\text{C=AsH}$, two complexes, that in which the metal cation is attached to the heteroatom and that in which it is attached to the carbon atom are local minima of the potential energy surface. Furthermore, as we shall discuss later, for the arsenic derivative the carbon attached species is the most stable one. We have considered it of interest to locate the transient species which connect both local minima. Their structures are given in Fig. 2. The important point is that while the isomerization barriers for the corresponding protonated species (see Fig. 3) are large enough as to make both isomers experimentally accessible, these barriers are much lower as far as the Cu^+ complexes are concerned, and therefore the carbon-attached and the heteroatom-attached structures can interconvert more easily.

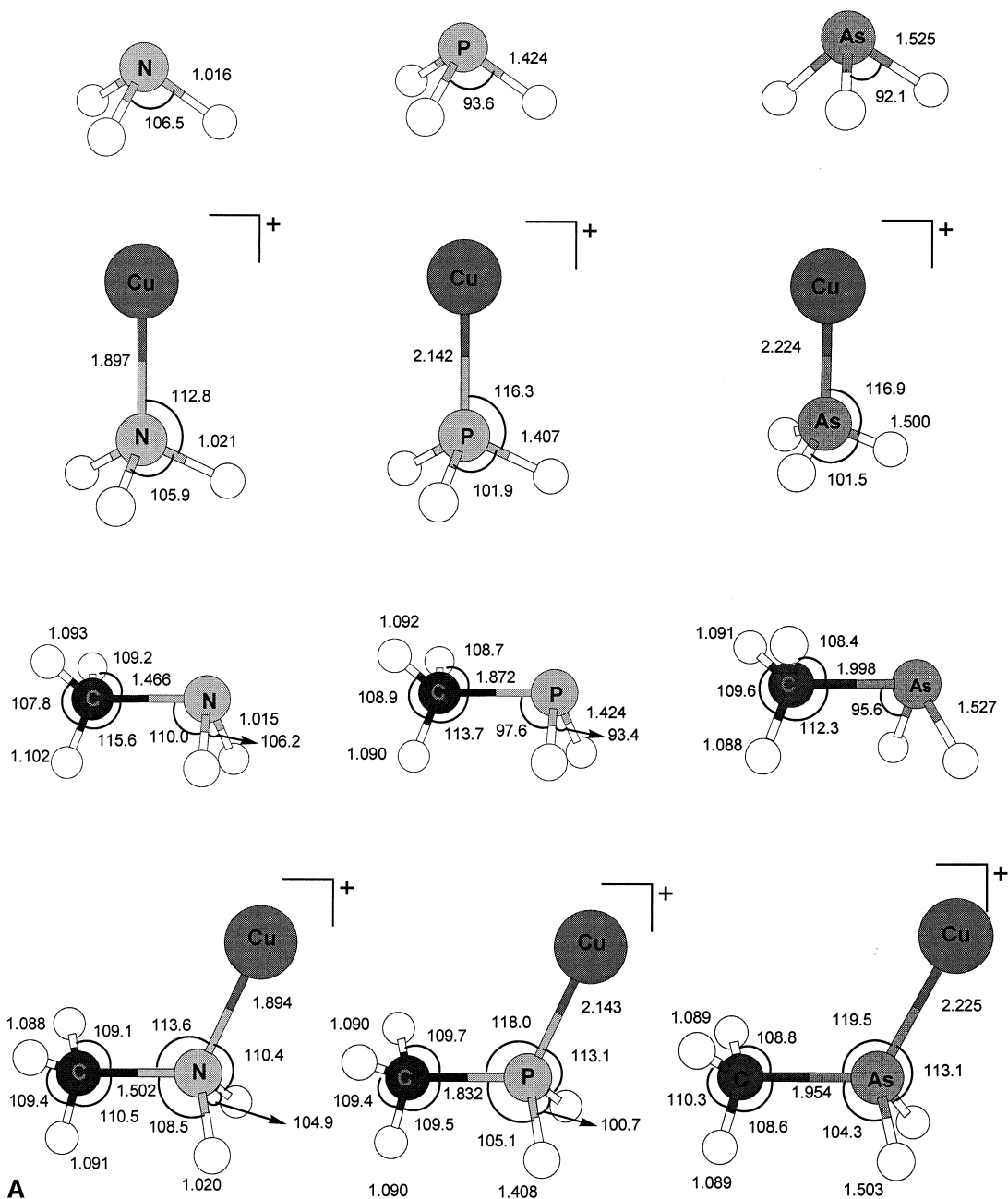


Fig. 1. B3LYP/6-311G(*d, p*) optimized geometries for the N, P, and As bases included in this study and their Cu⁺ complexes. For nitrogen containing systems the geometrical parameters were taken from [9]. Bond lengths are in angstroms and bond angles are in degrees.

It is worth noting that when Cu⁺ is attached to the carbon atom a ringlike structure is formed. However, an analysis of the topology of the charge densities of these three-membered rings indicates that no bond

critical point exists between the metal cation and the heteroatom, so these ringlike structures should be viewed as truly carbon attached species. To enhance the polarization interactions between the metal cation

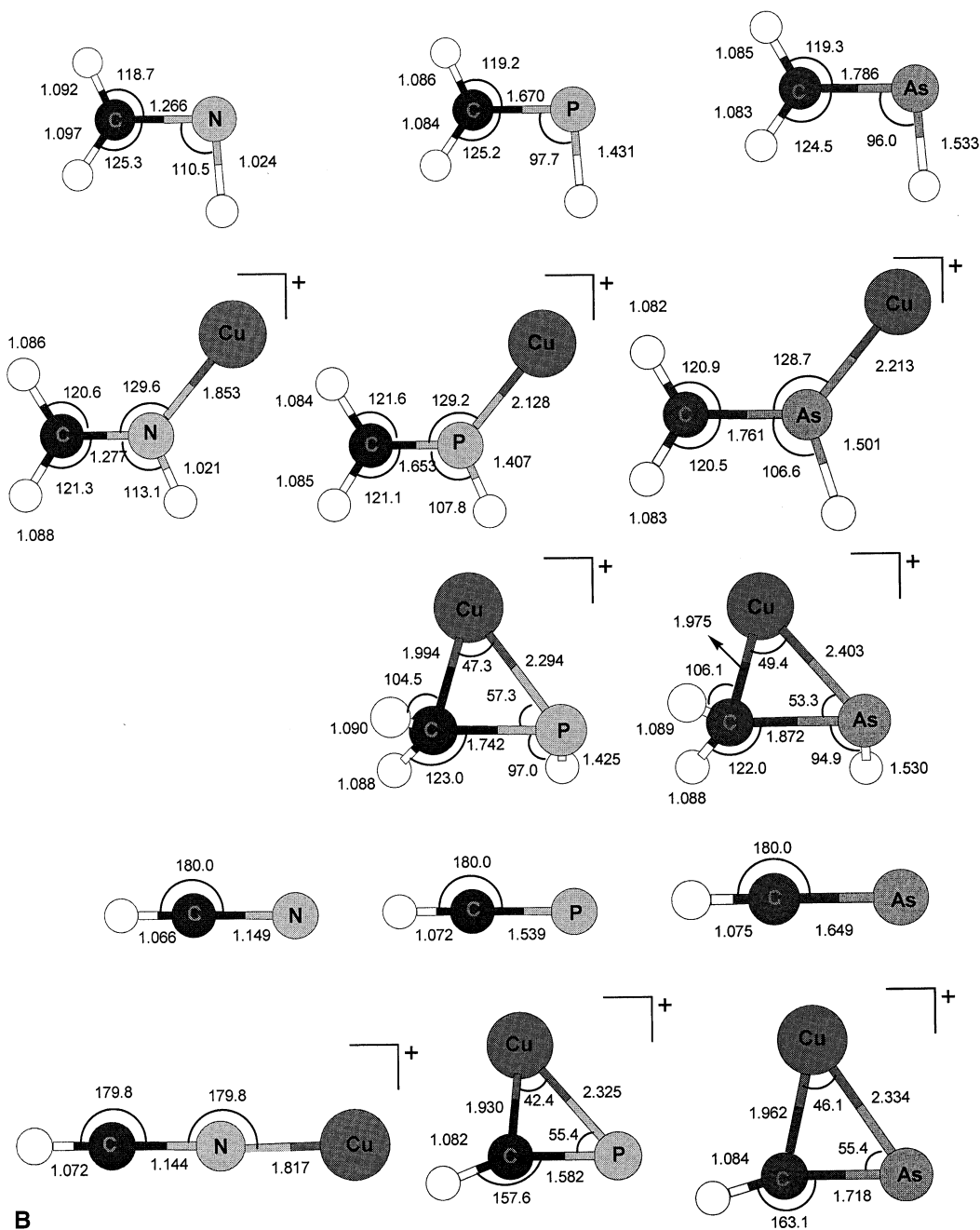


Fig. 1b.

and the heteroatom when this is P or As, the distance between both atomic centers becomes rather small, although no chemical bond is formed.

It can be also observed that the cationization of

the neutrals have also different structural effects. In H₂C=NH the C=N bond becomes weaker and longer upon Cu⁺ association. In contrast, when Cu⁺ is attached to P or As in H₂C=XH compounds, the C=X

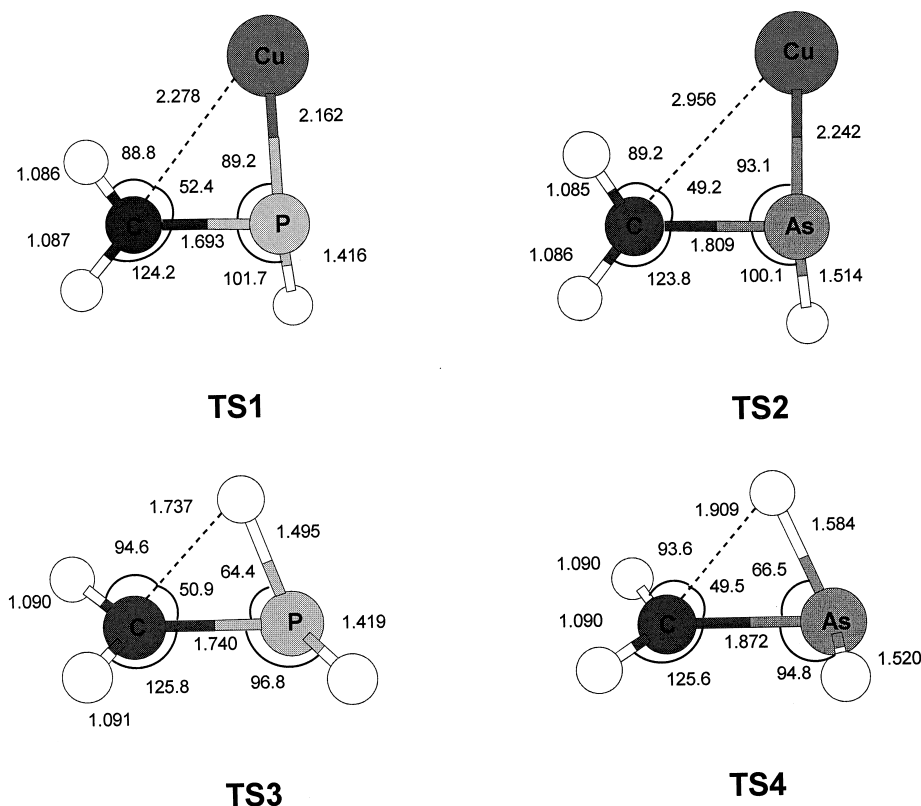


Fig. 2. B3LYP/6-311G(*d, p*) optimized geometries for the transition states connecting the heteroatom attached species and the carbon attached structures of the $\text{H}_2\text{C}=\text{XH}$ ($\text{X} = \text{P}, \text{As}, \text{Cu}^+$) complexes. Bond lengths in angstroms and bond angles in degrees.

bond becomes reinforced and shorter, and only when the metal cation is attached to the carbon atom the $\text{C}=\text{X}$ bond lengthens.

Obviously, the formation of the Cu^+ complex implies a significant charge transfer from the base to the metal cation. The important point is that the polarization undergone by the neutral base depends strongly on the electronegativity of the basic center. This has been already shown for the particular case of protonation processes by Alcamí et al. [22]. When a cation attaches to the atom which exhibits a larger electronegativity of the two atoms involved in a chemical bond, it recovers part of the charge transferred to the cation by depopulating the bonding region and, as a consequence, the bond is elongated and weakened. When the cation attaches to the less electronegative atom, it cannot depopulate the bond because of the presence of a more electronegative

partner, but it polarizes it. In this second case part of the electronic charge from the valence shell of the other atom moves into the bonding region reinforcing the linkage. Taking into account that nitrogen is more electronegative than carbon, while this is not the case for phosphorus and arsenic, it can be easily understood why nitrogen attachment is followed by a $\text{C}-\text{N}$ bond activation effect, while phosphorus (or arsenic) attachment is followed by a reinforcement of the $\text{C}-\text{P}$ (or $\text{C}-\text{As}$) bond (see Table 1). For the same reason, when the cation is attached to the carbon atom in P or As containing compounds, the $\text{C}-\text{P}$ or $\text{C}-\text{As}$ bonds become weaker.

Dissimilarities between nitrogen and phosphorus or arsenic compounds are also apparent as far as *sp* bases are concerned. While HCN yields only the nitrogen attached Cu^+ complex, for HCP and HCAs only the carbon attached species are stable.

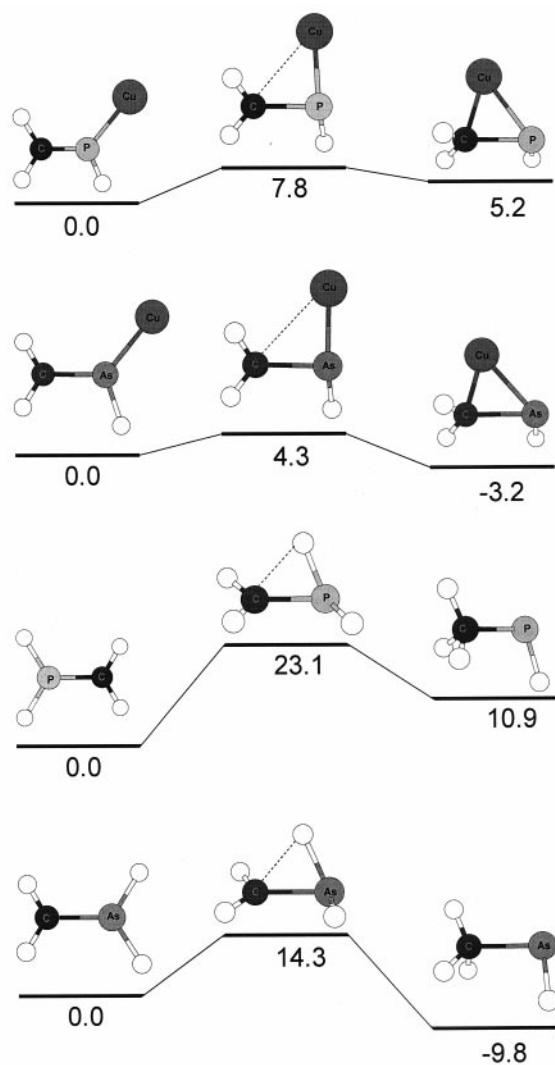


Fig. 3. Energy barriers connecting the heteroatom attached and the carbon attached complexes of $\text{H}_2\text{C}=\text{XH}$ ($\text{X} = \text{P}, \text{As}$) species. Values in kcal/mol obtained at the B3LYP/6-311 + G(3df, 2p) level of theory.

It is important to emphasize that the characteristics of the Cu^+ complexes resemble closely those of the corresponding protonated species (see Fig. 4). As it has been found for Cu^+ association, protonation of $\text{H}_2\text{C}=\text{NH}$ takes place exclusively at the nitrogen atom, and any attempt to obtain the carbon protonated species failed because the proton migrates toward the nitrogen atom without activation barrier. In contrast, $\text{H}_2\text{C}=\text{PH}$ and $\text{H}_2\text{C}=\text{AsH}$ protonate both at the heteroa-

tom and at the carbon atom. Furthermore, for the arsenic derivative the carbon protonated species is the most stable one. As mentioned above, the barriers connecting the heteroatom protonated structure and the carbon protonated form are sizably large (see Fig. 3).

For HCN only the nitrogen protonated species is a minimum of the potential energy surface, the carbon protonated species being a transition state, whose imaginary frequency corresponds to a rocking of the CH_2 group which would lead to the nitrogen protonated form. On the contrary, the phosphorus and arsenic analogs are only carbon bases in the gas phase.

The charge redistributions observed upon protonation are also qualitatively identical to those described above for the corresponding Cu^+ complexes, although quantitatively more intense, as reflected in the topology of the charge density as well as in the shifting of the corresponding stretching frequencies. Let us take the series $\text{H}_2\text{C}=\text{NH}$, $\text{H}_2\text{C}=\text{PH}$, $\text{H}_2\text{C}=\text{AsH}$ as an example. As illustrated in Table 1, nitrogen protonation or Cu^+ nitrogen attachment lead to a decrease of the charge density at the $\text{C}=\text{N}$ bond critical point, while the energy density becomes less negative. This decrease in the stabilizing charge concentration results in a lengthening of the bond and in a redshifting of the $\text{C}-\text{N}$ stretching frequency by 259 cm^{-1} for the protonated species and 17 cm^{-1} for the Cu^+ complex (see Table 2). On the contrary, protonation or Cu^+ association at the heteroatom in $\text{H}_2\text{C}=\text{PH}$ and $\text{H}_2\text{C}=\text{AsH}$ are accompanied by an increase of the charge density at the $\text{C}=\text{X}$ ($\text{X} = \text{P}, \text{As}$) bond critical point, while the energy density becomes more negative. Consistently, the bond shortens and the $\text{C}-\text{X}$ stretching frequency appears shifted to the blue. When the protonation or Cu^+ attachment in these two compounds take place at the carbon atom, the effects are the opposite. The charge density at the $\text{C}=\text{X}$ bond critical point decreases, the energy density becomes less negative, the bond lengthens and the $\text{C}-\text{X}$ stretching frequency appears redshifted.

3.2. Cu^+ binding energies and proton affinities

The total energies of the different species investigated in this study have been summarized in Table 3.

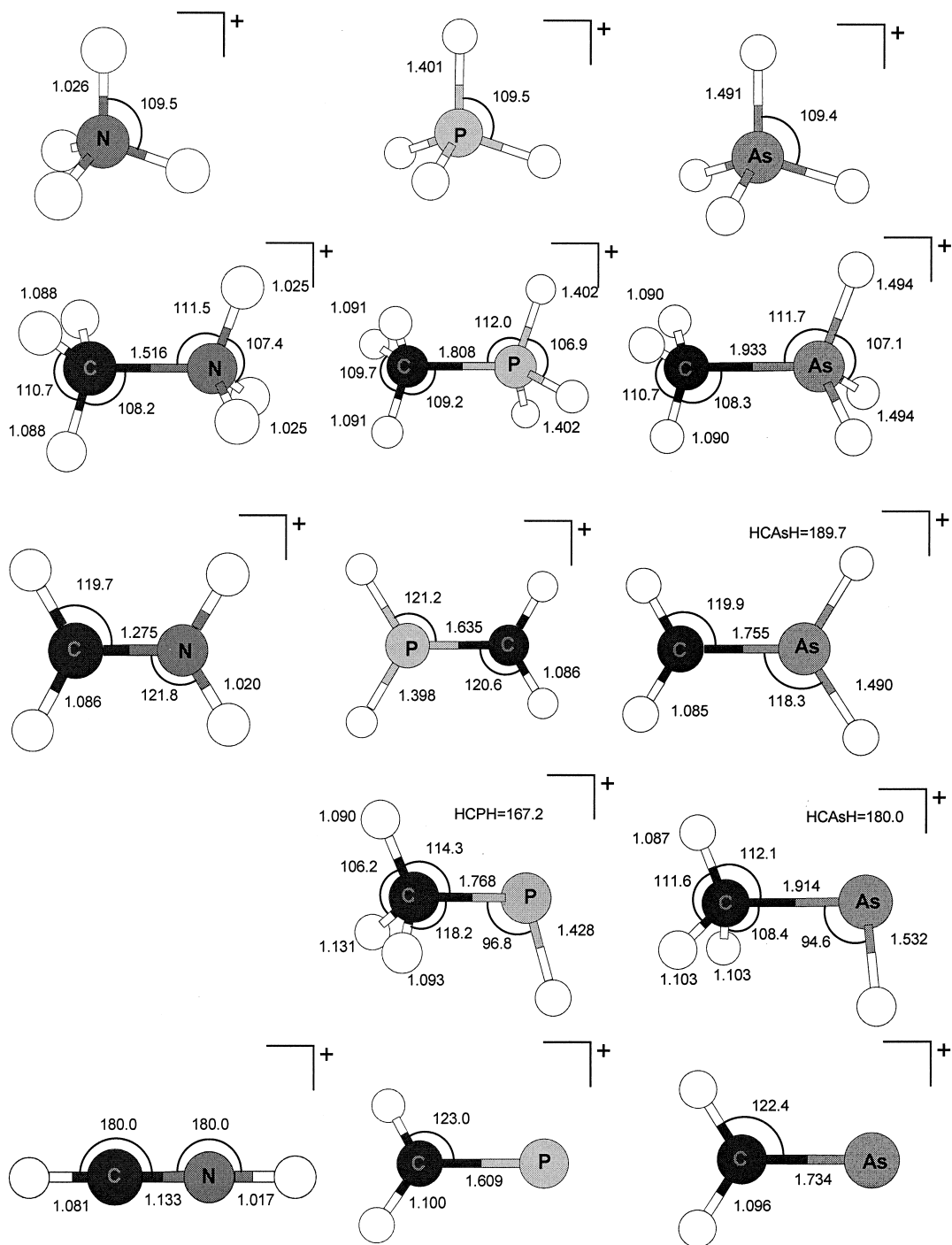


Fig. 4. B3LYP/6-311G(d, p) optimized geometries for the protonated forms of the neutral bases included in this study. Bond lengths in angstroms and bond angles in degrees.

Table 1

Charge densities (ρ) and energy densities [$H(r)$] evaluated at the corresponding bond critical points for $H_2C=XH$ ($X = N, P, As$) species, their protonated forms, and their Cu^+ complexes; all values are given in a.u. and have been calculated at the B3LYP/6-311G(*d, p*) level of theory

	Bond	Neutral		C-protonated		X-Protonated		C- Cu^+ complexes		X- Cu^+ complexes	
		ρ	$H(r)$	ρ	$H(r)$	ρ	$H(r)$	ρ	$H(r)$	ρ	$H(r)$
X = N	C–N	0.390	–0.621	0.371	–0.585	0.374	–0.588
	C–H	0.279	–0.274	0.292	–0.294	0.289	–0.287
	X–H	0.331	–0.419	0.333	–0.489	0.335	–0.455
X = P	C–P	0.187	–0.172	0.181	–0.188	0.203	–0.193	0.173	–0.164	0.195	–0.183
	C–H	0.279	–0.274	0.278	–0.271	0.281	–0.277	0.279	–0.272	0.282	–0.277
	X–H	0.161	–0.155	0.177	–0.184	0.180	–0.185	0.168	–0.167	0.172	–0.172
X = As	C–As	0.176	–0.130	0.152	–0.098	0.189	–0.147	0.154	–0.103	0.186	–0.142
	C–H	0.279	–0.275	0.280	–0.275	0.283	–0.280	0.278	–0.272	0.283	–0.280
	X–H	0.145	–0.103	0.156	–0.115	0.164	–0.129	0.151	–0.110	0.159	–0.121

This table includes also the ZPE corrections, the calculated Cu^+ binding energies and the proton affinities.

It can be observed that there is a very good agreement between our theoretical estimates for the proton affinities of PH_3 , H_3CPH_2 , HCP , and AsH_3 and the corresponding experimental values. Hence, we may safely assume that our estimates for the proton affinities of the unsaturated compounds, $H_2C=XH$ ($X = P, As$) and HCAs, would be also reliable. The very good agreement between the calculated and the experimental PA for HCP seems to ratify our conclusion that this compound is a carbon base in the gas phase. Also importantly, the Cu^+ binding energies for these two species obtained at the B3LYP/6-311 + G(2*df*, 2*p*) level are very close to the values estimated at the G2 level of theory. This can be taken as an indication of the reliability of this DFT approach to describe Cu^+ complexes when the basic center is a second or a third-row atom.

As it has been found before when discussing the

structures, there are also significant differences between the gas-phase reactivity of the nitrogen bases with respect to the phosphorus and arsenic analogs. In this respect it can be observed, for instance, that while the imine, $H_2C=NH$ is predicted to be a stronger base than ammonia, either when the reference acid is H^+ or Cu^+ , the $H_2C=PH$ compound is predicted to be less basic than PH_3 , both when the basic center is the phosphorus or the carbon atom. The corresponding arsenic derivative, $H_2C=AsH$ is less basic than arsine, AsH_3 , only when the cation attachment takes place at the arsenic atom. A rationalization of these basicity trends will be presented in forthcoming sections. In all cases the $H_2C=XH$ ($X = N, P, As$) derivatives are predicted to be the less basic compounds of all the series.

It is also worth noting that methyl substituent effects are quite different on going from nitrogen to phosphorus or arsenic containing compounds. As it can be deduced from the values in Table 3, these effects are significantly larger for phosphorus and

Table 2

C–X harmonic stretching frequencies (cm^{-1}) of $H_2C=XH$ ($X = N, P, As$) species, their protonated forms, and their Cu^+ complexes calculated at the B3LYP/6-311G(*d, p*) level of theory

	Neutral	C-protonated complexes	X-protonated complexes	C- Cu^+ complexes	X- Cu^+ complexes
$H_2C=NH$	1714	...	1455	...	1697
$H_2C=PH$	1001	821	1043	866	1033
$H_2C=AsH$	837	633	875	733	864

Table 3

B3LYP/6-311 + G(2df, 2p) total energies (E , in Hartrees), B3LYP/6-311G(d , p) zero point energy corrections (ZPE, in Hartrees), Cu^+ binding energies ($\text{Cu}^+ - \text{BE}$, in kcal/mol) and proton affinities (PA, in kcal/mol) for the different species under consideration

	E	ZPE	$\text{Cu}^+ - \text{BE}$		PA ^a	
			B3LYP ^b	G2 ^c	B3LYP ^b	Expt. ^d
$\text{Cu}-\text{NH}_3^+$	−1696.857 22	0.038 92	56.2 ^c	52.3		
$\text{Cu}-\text{NH}_2-\text{CH}_3^+$	−1736.175 78	0.067 97	59.8 ^c	59.0		
$\text{Cu}-\text{NH}=\text{CH}_2^+$	−1734.943 02	0.043 24	59.3 ^c	55.1		
$\text{Cu}-\text{NCH}^+$	−1733.717 12	0.017 79	50.0 ^c	46.7		
$\text{Cu}-\text{PH}_3^+$	−1983.442 72	0.027 32	53.4	52.2		
$\text{Cu}-\text{PH}_2-\text{CH}_3^+$	−2022.789 59	0.057 07	63.4			
$\text{Cu}-\text{PH}=\text{CH}_2^+$	−2021.531 80	0.035 44	52.9			
$\text{PH}=\text{CH}_2-\text{Cu}^+$	−2021.523 94	0.035 95	47.7			
$\text{Cu}-\text{HCP}^+$	−2020.293 03	0.015 37	47.0			
TS1	−2021.519 21	0.035 26	...			
$\text{Cu}-\text{AsH}_3^+$	−3877.932 44	0.024 75	49.5	47.5		
$\text{Cu}-\text{AsH}_2-\text{CH}_3^+$	−3917.277 40	0.054 45	58.5			
$\text{Cu}-\text{AsH}=\text{CH}_2^+$	−3916.018 89	0.033 86	48.1			
$\text{AsH}=\text{CH}_2-\text{Cu}^+$	−3916.024 61	0.034 61	51.3			
$\text{Cu}-\text{HCAs}$	−3914.791 37	0.014 58	51.8			
TS2	−3916.011 66	0.033 53	...			
NH_4^+	−56.923 11	0.049 46			201.8	204.0
NH_3CH_3^+	−96.254 42	0.079 16			213.0	214.9
NH_2CH_2^+	−95.011 49	0.054 09			206.4	203.8
HNCH^+	−93.739 97	0.027 89			168.8	170.4
PH_4^+	−343.484 80	0.035 18			185.7	187.6
PH_3CH_3^+	−382.844 01	0.065 22			203.3	203.5
PH_2CH_2^+	−381.566 47	0.042 40			181.2	
PHCH_3^+	−381.549 31	0.042 58			170.3	
H_2CP^+	−380.312 72	0.021 93			166.1	167.1
TS3	−381.528 11	0.040 80				
AsH_4^+	−2237.969 01	0.032 13			178.7	178.8
$\text{AsH}_3\text{CH}_3^+$	−2277.323 60	0.062 13			193.5	
$\text{AsH}_2\text{CH}_2^+$	−2276.046 14	0.039 90			172.3	
AsHCH_3^+	−2276.063 43	0.041 59			182.1	
H_2CAs^+	−2274.824 93	0.021 79			179.3	
TS4	−2276.022 08	0.038 62				
NH_3	−56.586 39	0.034 30				
NH_2-CH_3	−95.899 68	0.063 82				
$\text{NH}=\text{CH}_2$	−94.668 31	0.039 79				
NCH	−93.459 49	0.016 47				
PH_3	−343.177 50	0.023 86				
PH_2-CH_3	−382.509 08	0.054 29				
$\text{PH}=\text{CH}_2$	−381.268 90	0.033 54				
PCH	−380.040 00	0.013 98				
AsH_3	−2237.673 93	0.021 85				
AsH_2-CH_3	−2277.005 21	0.052 14				
$\text{AsH}=\text{CH}_2$	−2275.763 68	0.032 05				
AsCH	−2274.530 61	0.013 14				
Cu^+	−1640.176 69	0.000 00				

^a The calculated proton affinities are for the corresponding neutral compounds.

^b Binding energies at the B3LYP/6-311G(2df, 2p) level including ZPE correction.

^c For N-containing compounds the values have been taken from [9].

^d Experimental values of proton affinities taken from [2b].

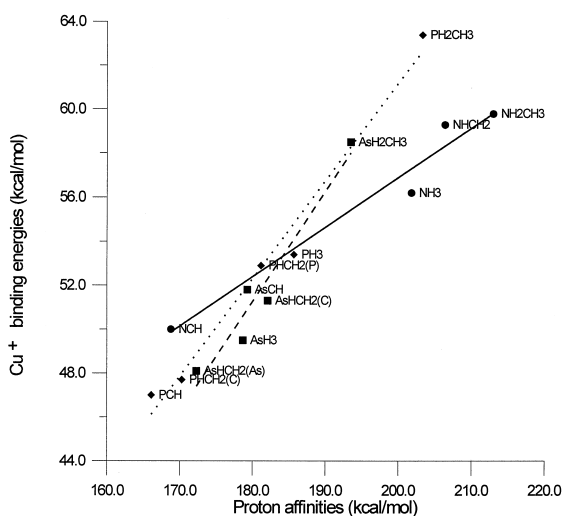


Fig. 5. Linear correlations between Cu^+ binding energies and proton affinities for nitrogen (continuous line), phosphorus (dotted line) and arsenic (dashed line) bases for $\text{H}_2\text{C}=\text{XH}$ ($\text{X} = \text{P}, \text{As}$) the basic center is indicated within parentheses. These linear correlations obey the following equations: nitrogen bases: $\text{Cu}^+-\text{BE} = 0.225 \text{ PA} + 11.89$ (kcal/mol), phosphorus bases: $\text{Cu}^+-\text{BE} = 0.444 \text{ PA} - 27.69$ (kcal/mol), arsenic bases: $\text{Cu}^+-\text{BE} = 0.500 \text{ PA} - 38.79$ (kcal/mol).

arsenic derivatives than for the nitrogen analog. Furthermore, this difference is more pronounced as far as Cu^+ binding energies are concerned. Actually, the effect of the methyl substitution on the proton affinity of phosphine is 1.5 times larger than that predicted for ammonia, while this factor becomes 2.7 for the corresponding Cu^+ binding energies.

As it has been reported before in the literature [4b] for other kinds of systems, there is apparently a rough correlation between the calculated Cu^+ binding energies and the corresponding proton affinities. However, a closer analysis of the data shows that nitrogen, phosphorus and arsenic containing bases follow different linear correlations (see Fig. 5). More importantly, while the slope of the correlations for phosphorus and arsenic compounds are rather similar, for nitrogen bases it is significantly different. The most important consequence is that although $\text{CH}_3\text{-PH}_2$ and $\text{CH}_3\text{-AsH}_2$ compounds have a smaller proton affinity than the nitrogen analog, their Cu^+ binding energies are sizably higher.

3.3. Reactivity trends

To gain some insight into the origin of the basicity trends discussed in the previous section we are going to analyze them for the particular case of the protonation processes, assuming that similar effects can be invoked for the corresponding Cu^+ binding energies. The first point which needs to be understood is why the unsaturated compounds are systematically less basic than the corresponding saturated counterparts. The second aspect that should be addressed is why $\text{H}_2\text{C}=\text{PH}$ behaves as a phosphorus base, while $\text{H}_2\text{C}=\text{AsH}$ behaves as a carbon base. A comparison of the relative stabilities of the saturated and unsaturated compounds with respect to the same reference compounds, for instance, the corresponding hydrocarbons can be a practical way to carry out such an analysis. The results obtained for nitrogen, phosphorus and arsenic derivatives have been schematized in Fig. 6.

Fig. 6 clearly illustrates that the origin of the basicity decrease of $\text{H}_2\text{C}=\text{NH}$ with respect to $\text{H}_3\text{C-NH}_2$ has a different origin than the similar decrease observed for phosphorus and arsenic compounds. In the first case the most significant changes take place in the neutral while in the other two cases take place in the protonated form. Let us discuss this in more detail. The upper part Fig. 6 indicates that for nitrogen bases a relative stabilization of the system takes place on going from the saturated to the unsaturated compound. In other words, the formation of a $\text{C}=\text{N}$ double bond by dehydrogenation of the corresponding saturated system is 6.1 kcal/mol less endothermic than the formation of a $\text{C}=\text{C}$ double bond by dehydrogenation of the saturated analog. In contrast for phosphorus and arsenic compounds the formation of $\text{C}=\text{P}$ or $\text{C}=\text{As}$ double bonds is slightly less favorable than the formation of $\text{C}=\text{C}$ bonds. This can be easily understood if one takes into account that multiple bonds between first and second (or third) row atoms are less stabilizing than those between first-row atoms.

The situation is just the opposite when the protonated species are considered. As illustrated by the lower part of the diagrams in Fig. 6, the formation of

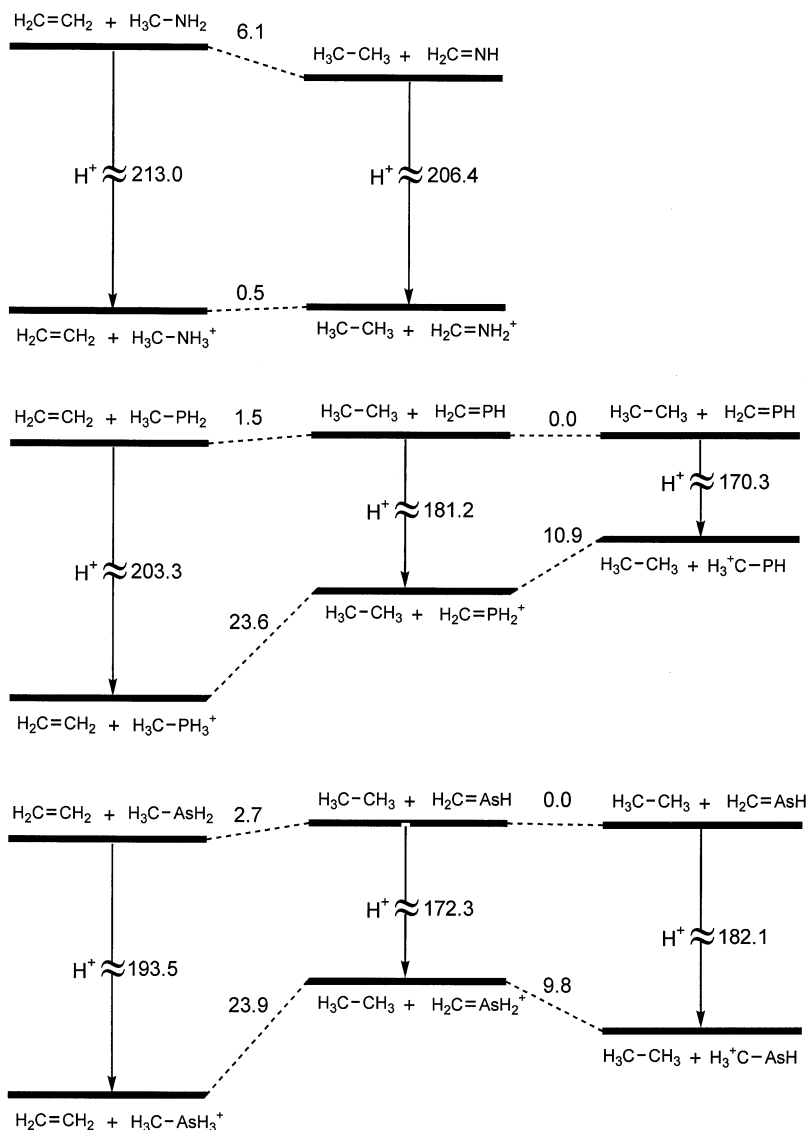


Fig. 6. Relative stability of $\text{C}=\text{X}$ ($\text{X} = \text{N}, \text{P}, \text{As}$) linkages as compared with $\text{C}=\text{C}$ bonds for both neutral $\text{H}_2\text{C}=\text{XH}$ species and their protonated forms. Values (in kcal/mol) obtained at the B3LYP/6-311 + G(2df, 2p) level of theory. These values include the corresponding ZPE corrections evaluated at the B3LYP/6-311G (d, p) level.

a double bond by the dehydrogenation of the corresponding saturated compound has a negligible effect (0.5 kcal/mol) on the relative stability of the system for nitrogen bases. For phosphorus and arsenic derivatives the same process implies a significant destabilization of the system by 23.6 and 23.9 kcal/mol, respectively. As a consequence, in the three cases, the

unsaturated compound is predicted to be less basic than the corresponding saturated analog. Why the dehydrogenation of $\text{H}_3\text{C}-\text{PH}_2$ requires much less energy than the dehydrogenation of the phosphorus protonated species? In both processes it is necessary to brake a $\text{C}-\text{H}$ bond and a $\text{P}-\text{H}$ bond and to change a $\text{C}-\text{P}$ bond into a $\text{C}=\text{P}$ one. Hence, three factors

Table 4

Charge densities (ρ), and energy densities [$H(\mathbf{r})$] evaluated at the corresponding bond critical points for the $\text{H}_3\text{C}-\text{XH}_2$ ($\text{X} = \text{N}, \text{P}, \text{As}$) species, their protonated forms, and their Cu^+ complexes; all values are given in a.u. and have been calculated at the B3LYP/6-311G(d, p) level of theory

	Bond	Neutral		Protonated		Cu^+ complexes	
		ρ	$H(\mathbf{r})$	ρ	$H(\mathbf{r})$	ρ	$H(\mathbf{r})$
$\text{X} = \text{N}$	C–N	0.262	−0.271	0.218	−0.248	0.234	−0.249
	C–H	0.272	−0.265	0.286	−0.284	0.282	−0.278
	X–H	0.373	−0.424	0.333	−0.471	0.336	−0.449
$\text{X} = \text{P}$	C–P	0.151	−0.143	0.175	−0.181	0.165	−0.165
	C–H	0.274	−0.270	0.275	−0.269	0.276	−0.270
	X–H	0.161	−0.155	0.180	−0.185	0.172	−0.171
$\text{X} = \text{As}$	C–As	0.127	−0.070	0.146	−0.087	0.139	−0.081
	C–H	0.275	−0.271	0.277	−0.272	0.277	−0.272
	X–H	0.146	−0.105	0.165	−0.129	0.158	−0.121

might be responsible of the aforementioned difference: either (1) the C–H bond is stronger in the protonated than in the neutral species, or/and (2) the P–H bond is stronger in the protonated than in the neutral species, or/and (3) the C=P bond in the protonated species is weaker than the C=P bond in the neutral, with respect to the C–P in the saturated analogs.

An analysis of the charge distribution of $\text{H}_3\text{C}-\text{PH}_2$ and its protonated form shows no significant changes in the charge densities and energy densities at the C–H bond critical points (see Table 4) upon protonation. Consistently, the C–H bond length remains

practically unchanged (see Fig. 1), as well as the C–H stretching frequencies (see Table 5). Therefore, we must conclude that factor (1) must play a negligible role. The same analysis, shows however, that, upon protonation, the charge density at the P–H bond critical points increase and the energy density becomes more negative. The expected reinforcement of the P–H bonds is mirrored in a decreasing of the bond length (see Fig. 1) and in a shifting of the P–H stretching frequencies to the blue (see Table 5). Factor (3) plays also a role, since according to our results the reinforcement of the C–P bond on going from the $\text{H}_3\text{C}-\text{PH}_2$ to the $\text{H}_2\text{C}=\text{PH}$ species is greater than on

Table 5

Stretching vibrational frequencies (cm^{-1}) for $\text{H}_3\text{C}-\text{XH}_2$ ($\text{X} = \text{N}, \text{P}, \text{As}$) species, their protonated forms, and their Cu^+ complexes calculated at the B3LYP/6-311G(d, p) level of theory

	Vibration	Neutral	Protonated	Cu^+ complexes
$\text{X} = \text{N}$	C–N Str.	1057	920	976
	C–H s. Str.	2948	3084	3064
	C–H a. Str.	3051	3185	3144
	N–H s. Str.	3487	3399	3456
	N–H a. Str.	3561	3472	3505
	C–P Str.	666	720	713
$\text{X} = \text{P}$	C–H s. Str.	3043	3051	3057
	C–H a. Str.	3116	3144	3147
	P–H s. Str.	2367	2512	2478
	P–H a. Str.	2373	2544	2487
	C–As Str.	552	598	588
	C–H s. Str.	3050	3060	3065
$\text{X} = \text{As}$	C–H a. Str.	3131	3165	3165
	As–H s. Str.	2180	2322	2283
	As–H a. Str.	2190	2354	2296

going from $\text{H}_3\text{C}-\text{PH}_3^+$ to $\text{H}_2\text{C}=\text{PH}_2^+$. Actually, in the first case the bond length shortens 0.202 Å and the charge density at the bond critical point increases 0.036 a.u., while in the latter it shortens only 0.173 Å and the charge density increases by 0.028 a.u. Hence, we must conclude that the reinforcement of the P–H bonds upon protonation and the fact that the C=P bond is weaker, in relative terms, in the protonated form than in the neutral form, are the main factors explaining the higher dehydrogenation energy of the protonated species. Entirely analogous effects are found for the corresponding arsenic derivatives (see Tables 4 and 5). The relative destabilization of the protonated form of the nitrogen bases, has a different origin. As shown in Tables 4 and 5, the N–H bonds become weaker rather than reinforced upon protonation, while the C–H linkages become reinforced. Concomitantly, the C=N linkage in the protonated species is stronger than in the neutral, relative to the saturated compound. Actually, it can be seen that on going from $\text{H}_3\text{C}-\text{NH}_2$ to $\text{H}_2\text{C}=\text{NH}$ the bond shortens 0.200 Å, while on going from $\text{H}_3\text{C}-\text{NH}_3^+$ to $\text{H}_2\text{C}=\text{NH}_2^+$ the shortening is 0.241 Å.

Let us now analyze the basicity changes on going from the phosphorus or arsenic protonated forms to the carbon protonated species. As illustrated in Fig. 6, this process is energetically disfavored for the phosphorus compound, but favorable for the arsenic derivative. To understand this difference, it must be taken into account that these are isomerization processes which involve a 1,2H shift. Accordingly, we are replacing a P–H (or As–H) bond by a C–H bond, which should lead to a stabilization of the system, and simultaneously a C=P (or C=As) bond is changed into a C–P (or C–As) bond, which would tend to destabilize the system. Therefore, two factors might explain the different behavior of phosphorus and arsenic derivatives: (1) a different strength of the double bonds (C=P or C=As) with respect to the single ones, and/or (2) a different strength of the P–H and As–H bonds with respect to the C–H linkages. The first factor can be analyzed using the type of reactions proposed by Pople and co-workers [23]:



$$\Delta H = -17.7 \text{ kcal/mol}$$



$$\Delta H = -18.9 \text{ kcal/mol}$$

which indicate that although the C=As bond is less stable, in relative terms, than a C=P bond, the stability difference, estimated at the B3LYP/6-311 + G(2df, 2p) level is rather small.

The difference is more pronounced as far as the relative stability of the P–H or As–H bonds with respect to the C–H bond, is concerned (see Table 6). The dissociation energies of these linkages can be easily obtained from the atomization energies of CH_4 , PH_3 , and AsH_3 , which can be reliably estimated at the G2 level of theory (see Table 6) and they show that the As–H linkages are about 7 kcal/mol weaker than P–H bonds. This result allows us to conclude that the enhanced stability of the carbon protonated species of the arsenic derivatives is mainly due to the net stabilization of the system when the As–H bond is replaced by a C–H linkage. In phosphorus compounds, this stabilization is smaller, and it is not enough to compensate the destabilization produced by changing a C=P double bond by a C–P single bond. In the light of our discussion in preceding sections, is reasonable to conclude, that similar arguments apply to the Cu^+ complexes.

Fig. 7 shows the relative energy changes on going from $\text{H}_2\text{C}=\text{XH}$ to $\text{HC}\equiv\text{X}$ systems. Again the behavior is different for nitrogen than for phosphorus or arsenic compounds, because the former behave as nitrogen bases, while the latter are carbon bases. It can be noted however, that, in relative terms, again the dehydrogenation of the protonated species is less favorable than that of the neutral systems for similar reasons to those explained above, and as a consequence the $\text{HC}\equiv\text{X}$ compounds are less basic than the $\text{H}_2\text{C}=\text{XH}$ analogs.

Table 6
X–H (X = C, N, P, H) dissociation energies (kcal/mol) estimated by using the atomization energies of the corresponding hydrides evaluated at the G2 level of theory

	CH	NH	PH	AsH
Bond energy	98.3	92.2	75.5	68.5

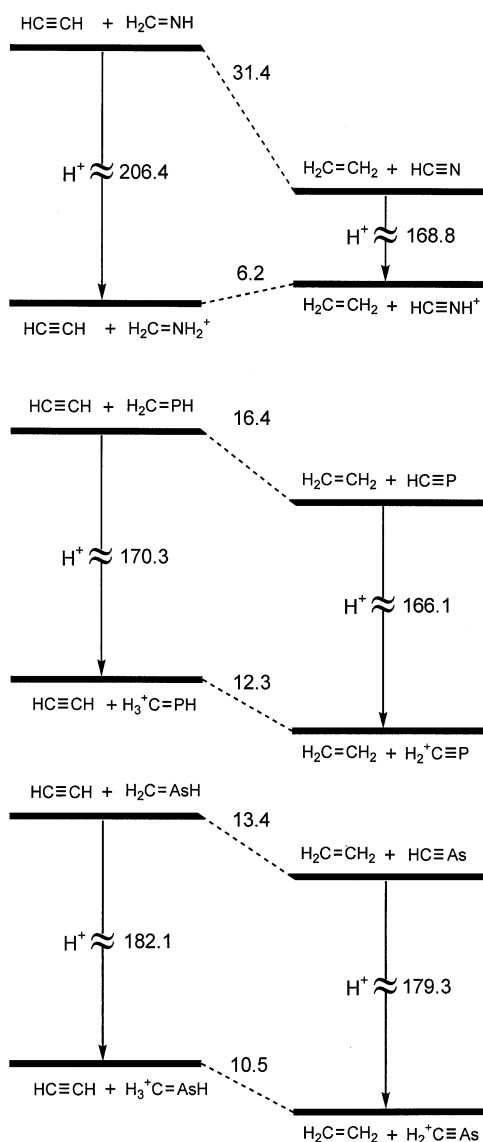


Fig. 7. Relative stability of C≡X (X = N, P, As) linkages as compared with C≡C bonds for both neutral HC≡X species and their protonated forms. Values (in kilocalories per mol.) obtained at the B3LYP/6-311 + G(2df, 2p) level of theory. These values include the corresponding ZPE corrections evaluated at the B3LYP/6-311G(d, p) level.

4. Conclusions

There exist significant differences in the reactivity trends of *sp*, *sp*², and *sp*³ nitrogen bases with respect to their phosphorus and arsenic analogs, both when

the reference acid is H⁺ or Cu⁺. In fact, our results show that proton affinities and Cu⁺ binding energies are linearly correlated, although the slope of the correlation for phosphorus and arsenic derivatives is significantly different from that of nitrogen bases. The main consequence is that, although the saturated phosphorus and arsenic compounds (H₃C–XH₂) have a smaller proton affinity than methylamine, their Cu⁺ binding energies are significantly higher.

The unsaturated systems are systematically less basic than the corresponding saturated counterparts. For phosphorus and arsenic derivatives this is mainly due to the reinforcement of the P–H or As–H bonds and to a relative destabilization of the C=X linkage upon protonation. For nitrogen compounds, is mainly due to a reinforcement of the C–H linkages and to a relative stabilization of the C=N bond. For H₂C=NH only the nitrogen attached species is stable. In contrast, for H₂C=PH and H₂C=AsH compounds both, the species in which the cation is bonded to the heteroatom or to the carbon atom are local minima of the potential energy surface. Furthermore, for the arsenic derivative the latter is the most stable form. This difference between phosphorus and arsenic compounds is a consequence of the different relative strength of the P–H bonds with respect to the As–H bonds, since, surprisingly, the C=As bonds exhibit a relative stability quite similar to that of the C=P linkages.

For HCN only the nitrogen attached species is stable, while for HCP and HCAs only the carbon attached structures are found.

Methyl substituent effects for phosphorus and arsenic compounds are systematically larger than for the corresponding nitrogen derivative. These differences are more pronounced in Cu⁺ complexes than in protonated structures.

The observed differences in the aforementioned reactivity trends reflect significant dissimilarities in the charge redistribution undergone by the neutral when it interacts with the attaching ion. This is a direct consequence of the fact that while nitrogen is more electronegative than hydrogen and carbon, phosphorus and arsenic are not. This is clearly re-

flected in the optimized geometries and in the shift-
ings of the harmonic stretching frequencies.

Finally, it is worth to emphasize that the B3LYP
method, when used with a flexible enough basis set,
can be a reliable alternative to high level ab initio
calculations, for the theoretical treatment of, not only
first-row, but also second- and third-row containing
compounds.

Acknowledgements

This work has been partially supported by the
DGES project no. PB96-0067. A generous allocation
of computational time at the CCCFC of the Univer-
sidad Autónoma de Madrid is also gratefully ac-
knowledged. One of the authors (A.L.) also acknowl-
edges a postdoctoral contract from the Ministerio de
Educación y Cultura of Spain.

References

- [1] See for instance, (a) R.W. Taft, R.D. Tompson, *Prog. Phys. Org. Chem.* 16 (1987) 1; (b) *Gas-phase Ion Chemistry*, M.T. Bowers (Ed.), Academic, New York, 1979, Vols. 1 and 2; 1984, Vol. 3, and references therein.
- [2] (a) S.G. Lias, J.E. Bartmess, J.F. Liebman, J.L. Holmes, R.D. Levine, W.J. Mallard, *J. Phys. Chem. Ref. Data* 17 (1988) suppl. 1; (b) E.P. Hunter, S.G. Lias, *J. Phys. Chem. Ref. Data* 27 (1998) 413.
- [3] See for instance, (a) *Organometallic Ion Chemistry*; B.S. Freiser (Ed.), Kluwer Academic, Dordrecht, 1995; (b) P.B. Armentrout, T. Baer, *J. Phys. Chem.* 100 (1996) 12866; (c) B.S. Freiser, *J. Mass Spectrom.* 31 (1996) 70, and references therein.
- [4] (a) R.L. Woodin, F.A. Houle, W.A. Goodard III, *Chem. Phys.* 14 (1976) 6520; (b) R.W. Jones, R.H. Staley, *J. Am. Chem. Soc.* 104 (1982) 2296; (c) J.F. Gal, R.W. Taft, R.T. McIver *Spectros. Int. J.* 3 (1984) 96; (d) M. Alcamí, O. Mó, M. Yáñez, F. Anvia, R.W. Taft, *J. Phys. Chem.* 94 (1990) 4796.
- [5] See for instance, (a) G. Bouchoux, J.P. Flament, Y. Hoppiliard, J. Tortajada, R. Flammang, A. Maquestiau, *J. Am. Chem. Soc.* 111 (1989) 5560; (b) A. Luna, M. Yáñez, *J. Phys. Chem.* 97 (1993) 10659; (c) A.P. Scott, R.H. Nobes, H.F. Schaefer III, L. Radom, *J. Am. Chem. Soc.* 116 (1994) 10159; (d) J.R. Flores, C. Barrientos, A. Largo, *J. Phys. Chem.* 98 (1994) 1090; (e) E.W.-G. Diau, S.C. Smith, *J. Phys. Chem.* 100 (1996) 12349; (f) P.M. Mayer, L. Radom, *Chem. Phys. Lett.* 280 (1997) 244; (g) N. Marchand, P. Jimeno, J.C. Rayez, D. Liotard, *J. Phys. Chem. A* 101 (1997) 6077; (h) A.J. Chalk, L. Radom, *J. Am. Chem. Soc.* 119 (1997) 7573; (i) Q. Chen, B.S. Freiser, *Chem. Phys. Lett.* 284 (1998) 339; (j) D. Stöckigt, *J. Phys. Chem. A* 102 (1998) 10493; (k) S.S. Yi, M.R.A. Blomberg, P.E.M. Siegbahn, J.C. Weisshaar, *ibid.* 102 (1998) 395; (l) A. Irigoras, J.E. Fowler, J.M. Ugalde, *ibid.* 102 (1998) 293; (m) A. Irigoras, J.E. Fowler, J.M. Ugalde, *J. Am. Chem. Soc.* 121 (1999) 574.
- [6] See for instance, (a) P. Redondo, A. Largo, C. Barrientos, J.M. Ugalde, *J. Phys. Chem.* 95 (1991) 4318; (b) R.H. Nobes, L. Radom, *Chem. Phys. Lett.* 189 (1992) 554; (c) J.S. Francisco, Y. Zhao, W.A. Lester Jr., I.H. Williams, *J. Chem. Phys.* 96 (1992) 2861; (d) T.S. Dibble, J.S. Francisco, *ibid.* 99 (1993) 397; (e) M. Esseffar, A. Luna, O. Mó, M. Yáñez, *Chem. Phys. Lett.* 209 (1993) 557; (f) A.L.L. East, W.D. Allen, *J. Chem. Phys.* 99 (1993) 4638; (g) J.S. Francisco, *J. Chem. Phys.* 99 (1993) 10082; (h) C.F. Rodriguez, A.C. Hopkinson, *J. Phys. Chem.* 97 (1993) 849; (j) C.W. Bauschlicher Jr., H. Partidge, *ibid.* 98 (1994) 1826; (k) T.S. Dibble, J.S. Francisco, *ibid.* 98 (1994) 11694; (l) A. Luna, M. Manul, O. Mó, M. Yáñez, *ibid.* 98 (1994) 6980; (m) F. Grandinetti, A. Ricci, *Chem. Phys. Lett.* 253 (1996) 189.
- [7] (a) M. Alcamí, O. Mó, M. Yáñez, *J. Phys. Chem.* 93 (1989) 3929; (b) M. Alcamí, O. Mó, J.L.G. De Paz, M. Yáñez, *Theoret. Chim. Acta* 77 (1990) 1; (c) M. Alcamí, O. Mó, M. Yáñez, *J. Phys. Chem.* 96 (1992) 3022; (d) J. Tortajada, A. Total, J.P. Morizur, M. Alcamí, O. Mó, M. Yáñez, *ibid.* 96 (1992) 8309; (e) O. Mó, M. Yáñez, A. Total, J. Tortajada, J.P. Morizur, *ibid.* 97 (1993) 5553; (f) M. Alcamí, O. Mó, M. Yáñez, *J. Am. Chem. Soc.* 115 (1993) 11074; (g) J. Tortajada, E. Leon, A. Luna, M. Yáñez, *J. Phys. Chem.* 98 (1994) 12919; (h) J. Tortajada, E. Leon, J.-P. Morizur, A. Luna, M. Yáñez, *ibid.* 99 (1995) 13890; (i) E. Leon, B. Amekraz, J. Tortajada, J.-P. Morizur, A.I. González, O. Mó, M. Yáñez, *ibid.* 101 (1997) 2489.
- [8] (a) A. Luna, B. Amekraz, J.-P. Morizur, J. Tortajada, O. Mó, M. Yáñez, *J. Phys. Chem.* 101 (1997) 5931; (b) A. Luna, B. Amekraz, J. Tortajada, J.-P. Morizur, M. Alcamí, O. Mó, M. Yáñez, *J. Am. Chem. Soc.* 120 (1998) 5411; (c) A. Luna, J. Tortajada, J.-P. Morizur, M. Alcamí, O. Mó, M. Yáñez, *J. Phys. Chem.* 102 (1998) 4652; (d) M. Alcamí, O. Mó, M. Yáñez, A. Luna, J. Tortajada, J.-P. Morizur, *ibid.* 102 (1998) 10120.
- [9] A. Luna, B. Amekraz, J. Tortajada, *Chem. Phys. Lett.* 266 (1997) 31.
- [10] GAUSSIAN-94, Revision B. 1, M.J. Frisch, G.W. Trucks, H.B. Schlegel, P.M.W. Gill, B.G. Johnson, M.A. Robb, J.R. Cheeseman, T.A. Keith, G.A. Peterson, J.A. Montgomery, K. Raghavachari, M.A. Al-Laham, V.G. Zakrzewski, J.V. Ortiz, J.B. Foresman, J. Ciolowski, B.B. Stefanow, A. Nanayaklara, M. Challacombe, C.Y. Peng, P.Y. Ayala, W. Chen, M.W. Wong, J.L. Andres, E.S. Replogle, R. Gomperts, R.L. Martin, D.J. Fox, J.S. Binkley, D.J. Defrees, J. Baker, J.P. Stewart, M. Head-Gordon, C. González, J.A. Pople, Gaussian, Inc., Pittsburgh, PA, 1995.
- [11] (a) J. Florián, B.G. Johnson, *J. Phys. Chem.* 98 (1994) 3681; (b) C.W. Bauschlicher, *Chem. Phys. Lett.* 246 (1995) 40; (c) J.M. Martell, J.D. Goddard, L.A. Erikson, *J. Phys. Chem.* 101 (1997) 1927; (d) Q. Cui, D.G. Musaev, M. Svensson, D. Sieber, K. Morokuma, *J. Am. Chem. Soc.* 117 (1995) 12366;

- (e) A. Ricca, C.W. Bauschlicher, J. Phys. Chem. 99 (1995) 9003; (f) T. Ziegler, Chem. Rev. 91 (1991) 651.
- [12] S. Hoyau, G. Ohanessian, Chem. Phys. Lett. 280 (1997) 266.
- [13] (a) A.D. Becke, J. Chem. Phys. 98 (1993) 5648. (b) 96 (1992) 2155.
- [14] C. Lee, W. Yang, R.G. Parr, Phys. Rev. B 37 (1988) 785.
- [15] (a) A.J.H. Watchers, J. Chem. Phys. 52 (1970) 1033. (b) P.J. Hay, *ibid.* 66 (1977) 4377.
- [16] L.A. Curtiss, K. Raghavachari, G.W. Trucks, J.A. Pople, J. Chem. Phys. 94 (1991) 7221.
- [17] D. Walter, P.B. Armentrout, J. Am. Chem. Soc. 120 (1998) 3176.
- [18] L.A. Curtiss, M.P. McGrath, J.-P. Blaudeau, N.E. Davis, R.C. Binning, Jr., L. Radom, J. Chem. Phys. 103 (1995) 6104.
- [19] J.A. Pople, M. Head-Gordon, D.J. Fox, K. Raghavachari, L.A. Curtiss, J. Chem. Phys. 90 (1989) 5622.
- [20] R.F.W. Bader, *Atoms in Molecules. A Quantum Theory*, Oxford University Press, Oxford, 1990.
- [21] The AIM-PAC programs package has been provided by J. Cheeseman and R.F.W. Bader.
- [22] M. Alcamí, O. Mó, M. Yáñez, J.L-M. Abboud, J. Elguero, Chem. Phys. Lett. 172 (1990) 471.
- [23] W.J. Hehre, L. Radom, P.v.R. Schleyer, J.A. Pople, *Ab Initio Molecular Orbital Theory*, Wiley, New York, 1986.